AD-785 646

DETERMINATION OF AIRCRAFT CABIN RADIATION, CONDUCTION, AND CONVECTION HEAT TRANSFER COEFFICIENTS

Emmett J. Laing

Army Aviation Systems Test Activity
Edwards Air Force Base, California

1974

DETERMINATION OF AIRCRAFT CABIN RADIATION, CONDUCTION, AND CONVECTION HEAT TRANSFER COEFFICIENTS

Emmett J. Laing
United States Army Aviation Systems Test Activity
Edwards Air Force Base, California

NOTATION

A	Aircraft cabin transparent area, ft^2
C	Heat capacity, BTU/°F-ft^2
E_{ex}	Total external radiation, BTU/hr-ft^2
E_s	Solar radiation, BTU/hr-ft^2
K_c	Conduction heat transfer coefficient, °F-hr-ft^2/BTU
K_r	Radiation heat transfer coefficient, °F-hr-ft^2/BTU
T_a	Ambient air temperature, °R
T_c	Transient aircraft cabin temperature, °R
T_o	Initial aircraft cabin temperature, °R
T_{ss}	Steady-state aircraft cabin temperature, °R
t	Time, hr
V	Aircraft cabin volume, ft^3
σ	Stefan-Boltzman constant, BTU/hr-ft^2-$°R^4$

15

INTRODUCTION

To properly design aircraft instruments, avionics, and other equipment, which is installed in aircraft cabin areas, it is necessary to accurately know the cabin temperature environment. Aircraft cabin temperatures vary widely depending on the aircraft operating condition, basic design parameters, and type of environmental control system installed. Previous tests at the United States Army Aviation Systems Test Activity (USAASTA) have shown that the highest cabin temperatures frequently occur with the aircraft static in an environment with both high solar radiation and high ambient air temperatures (refs 1 through 5). It is suspected that high aircraft cabin static temperatures may increase aircraft component failure rates, cause equipment to temporarily malfunction, and directly cause equipment failure. However, accurate temperature data for the static environment are not available for many aircraft. To obtain this type of data, USAASTA, with the assistance of the United States Army Air Mobility Research and Development Laboratory, Eustis Directorate, has conducted comprehensive static temperature surveys on five first-line United States Army helicopters.

Lack of readily available test chamber facilities, which would allow a closely controlled environmental test, dictated the use of the available natural environment. To increase the accuracy of performing static temperature testing under natural conditions, a test method was developed which allowed the determination of combined conduction, convection, and radiation heat transfer coefficients for an aircraft cabin. Once these coefficients have been determined, the cabin static temperatures can be calculated for any natural conditions, allowing comparison of data gathered at different conditions and standardization of data to identical environmental conditions. References 1 through 5 are the formal published USAASTA reports from which the static temperature data in this paper are taken. It is anticipated that the test method and data presented in this paper will play an important role in the conduct of future static temperature testing, and increase the understanding and control of the aircraft cabin static temperature environment.

AIRCRAFT CABIN STATIC TEMPERATURES

Table 1 lists the physical characteristics of the helicopters tested pertinent to the heat transfer properties of the cabin. The most significant characteristic applicable to the static temperature environment is the ratio of cabin transparent area to cabin volume. In general, the larger the area-to-volume ratio, the higher the cabin static temperature will be. Figures 1 and 2 show photographs of two United States Army helicopters with large amounts of transparent area which are present for maximum visibility. The transparent area in all of the helicopters tested is plastic, with the approximate radiation transmissibility characteristics shown in figure 3. These characteristics, together with cabin closure, result in the so-called "greenhouse" effect, which allows solar radiation to increase cabin temperatures above the ambient air temperature. Figure 4 shows the

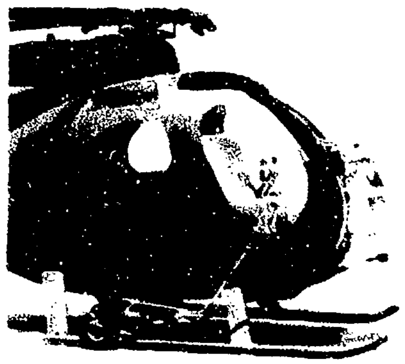

Figure 1. OH-6A Helicopter.

Figure 2. AH-1G Helicopter.

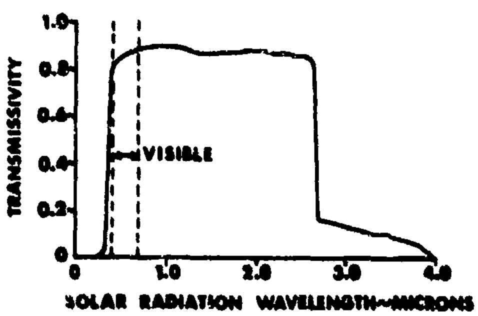

Figure 3. Typical Transmissivity for Aircraft Transparent Area.

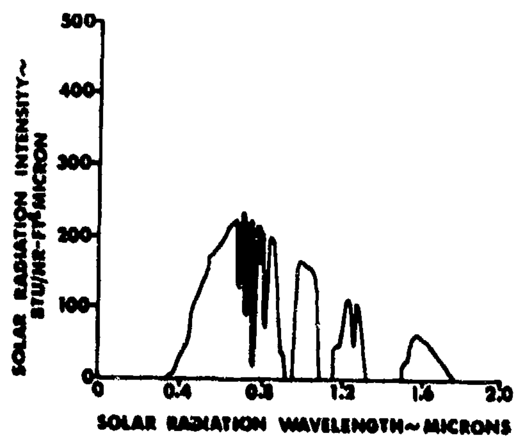

Figure 4. Typical Solar Radiation at at the Earth's Surface.

solar radiation spectral distribution at the earth's surface. As shown in figure 3, the plastic is transparent to the solar radiation, which, after it passes through the plastic, is both absorbed, reemitted, and reflected by the cabin equipment and internal structure. The reflected radiation exits the cabin through the plastic but the absorbed radiation is reemitted at a lower temperature and longer wavelengths, to which the plastic is not transparent. Thus the transparent areas in effect trap reemitted solar radiation in the cabin and cause the cabin temperature to rise until the heat loss rate by means of cabin skin conduction to the atmosphere and cabin surface radiation is equal to the heat gain rate from solar radiation.

Figure 5 presents solar radiation data for the continental United States for maximum values during the winter and summer (ref 6). These data can be used to determine the solar radiation environment to which aircraft are subjected and to determine environmental test conditions and test geographical locations. Only a limited amount of world-wide solar radiation data are available (refs 7 and 8); however, the available data indicate that the maximum solar radiation values obtained in the continental United States are as severe as those obtained anywhere else in the world. The highest solar radiation values in the United States generally occur in the western high desert areas. Current United States Army tactics consider operation in the environments of Central Europe and Central Asia. As a matter of reference, the solar radiation and temperature environments of the Federal Republic of Germany and of Iran approximate the environments of the New England and western desert regions of the United States, respectively.

Table 1. Physical Characteristics.

Designation	Profile	Maximum Weight (lb)	Cabin Glass Area (ft^2)	Cabin Volume (ft^3)	Cabin Transparent Area to Cabin Volume Ratio
OH-58A	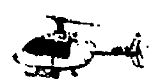	3,000	33.9	121	.28
OH-6A		2,700	46.3	100	.46
UH-1H		9,500	68.2	516	.13
AH-1G		9,500	51.9	95.9	.54
CH-54B		47,000	52.2	421	.12

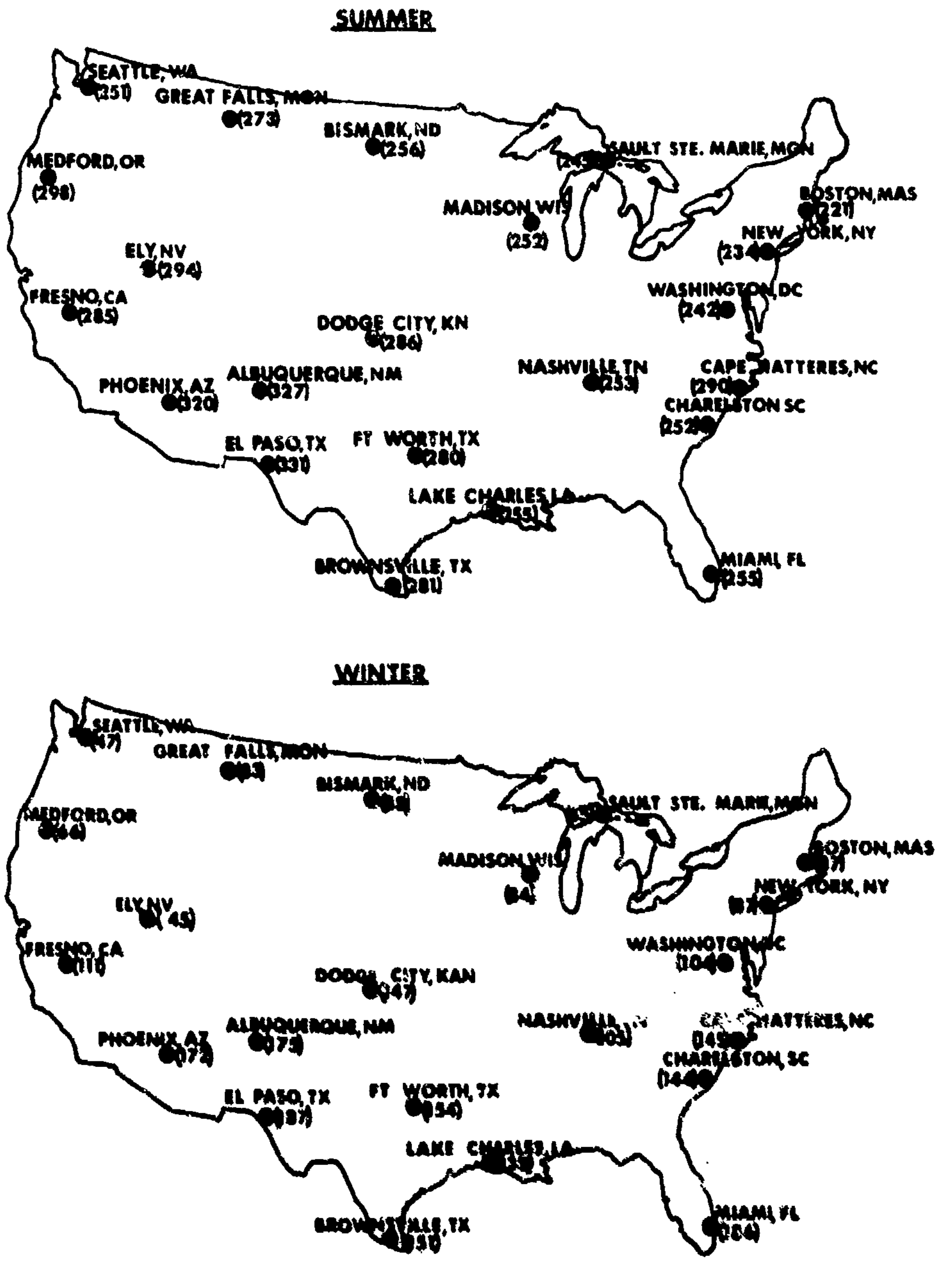

Figure 5. Continental Solar Radiation, Maximum Daily Values, BTU/hr-ft^2 (Ref 6).

A typical seasonal variation of solar radiation is shown in figure 6. The data indicate that test conditions at maximum solar radiation values may only be obtained during the months of April to July in the western desert areas. In addition to high solar radiation, a high ambient air temperature is also required for static temperature testing. The combination of high static temperatures and high solar radiation does not consistently occur. A test chamber may be used to artificially create the desired solar radiation and temperature environment; and static testing of many material items has been conducted in test chambers. However, test chambers do not always accurately reproduce the natural environment (ref 9) and are not easily available for static aircraft testing.

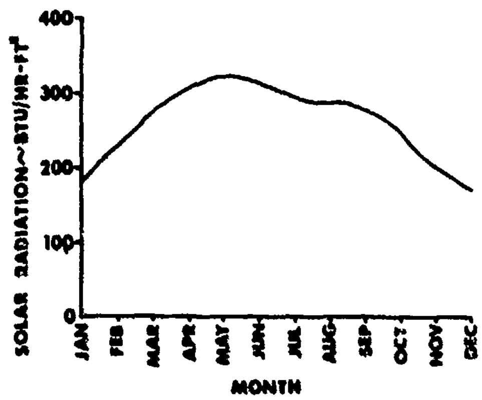

Figure 6. Monthly Variation of Solar Radiation - Phoenix, Arizona (Ref 6).

AIRCRAFT CABIN ELECTRICAL ANALOG

The electrical analog shown in figure 7 represents an aircraft cabin under static heating conditions. The voltage and current sources represent ambient air temperature and total external radiation, respectively. The capacitor represents the aircraft cabin and the two resistors represent cabin heat transfer coefficients. Using the circuit shown in figure 7, the equation describing the transient response of the aircraft cabin to an ambient air temperature and a source of external radiation can be written as:

$$T_c = \left[e^{-t/K_{eq}C}\right]\left[T_o - \frac{T_a K_r + E_{ex} K_c K_r}{K_c + K_r}\right] + \frac{T_a K_r + E_{ex} K_c K_r}{K_c + K_r} \qquad (1)$$

Where: $K_{eq} = \dfrac{K_c K_r}{K_c + K_r}$

ELECTRICAL QUANTITY	HEAT TRANSFER QUANTITY	UNIT
V - Voltage	T_a - Ambient air temperature	°R
V_c - Voltage across capacitor	T_c - Transient temperature inside helicopter	°R
	T_{ss} - Steady-state temperature inside helicopter	°R
	T_o - Initial temperature inside helicopter	°R
R_1 - Resistance	K_c - Radiation heat transfer coefficient	°F-hr-ft^2/BTU
R_2 - Resistance	K_r - Radiation heat transfer coefficient	°F-hr-ft^2/BTU
C - Capacitor	C - Heat capacity	BTU/°F-ft^2
I - Current	E_{ex} - Total external radiation	BTU/hr-ft^2
	E_a - Atmospheric radiation (total external radiation minus solar radiation)	BTU/hr-ft^2
	E_s - Solar radiation	BTU/hr-ft^2
t - Time	t - Time	Hr

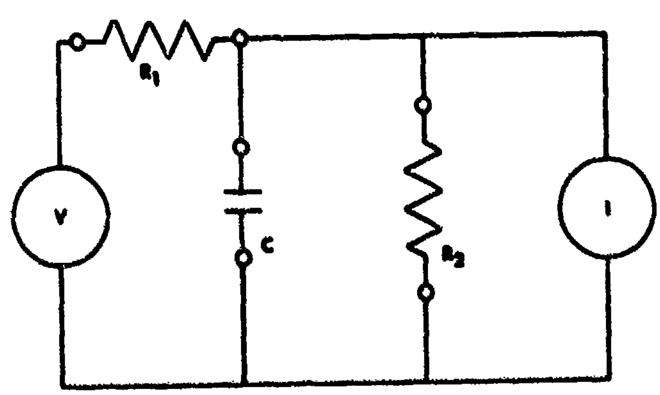

Figure 7. Aircraft Cabin Electrical Analog.

When t (time) $\rightarrow \infty$ the steady-state helicopter temperature T_{ss} is given by

$$T_{ss} = \frac{T_a K_r + E_{ex} K_c K_r}{K_c + K_r} \qquad (2)$$

Where: $E_{ex} = E_s + \sigma T_a^4$

$\sigma = 1.714 \times 10^{-9}$ BTU/ft²-HR-°R⁴

Total external radiation is the sum of solar radiation and the radiation emitted by the surrounding environment. The surrounding environment emits radiation in accordance with the Stefan-Boltzman law shown in equation 3.

Equation 2 is used to find K_c and K_r by allowing the aircraft to reach its steady-state temperature at two different constant ambient air temperatures (T_{a_1} and T_{a_2}) and at two different constant external radiation values (E_{ex_1} and E_{ex_2}). This results in two equations with two unknowns, K_c and K_r, which are solved for K_c and K_r in equations 4 and 5. A different K_c and K_r are calculated for each temperature sensor location. A convection coefficient is not calculated, and any convection effects are combined with the conduction and radiation coefficients.

$$K_c = \frac{T_{a_2} T_{ss_1} - T_{a_1} T_{ss_2}}{E_{ex_1} T_{ss_2} - E_{ex_2} T_{ss_1}} \qquad (4)$$

$$K_r = \frac{T_{ss_1} K_c}{T_{a_1} + E_{ex_1} K_c - T_{ss_1}} \qquad (5)$$

TEST METHODS

It was found that the helicopters tested required about 2 hours to reach steady-state temperatures. This relatively long stabilization time meant that the test could only be conducted at mid-day when solar radiation is nearly constant for a 2-hour period (fig. 8). The second value of solar radiation was obtained by allowing the aircraft to set all night and taking readings just before sunrise. At this time of day, measured solar radiation is negative and the aircraft cabin is slightly cooler than the ambient air temperature, since it is losing heat by radiation.

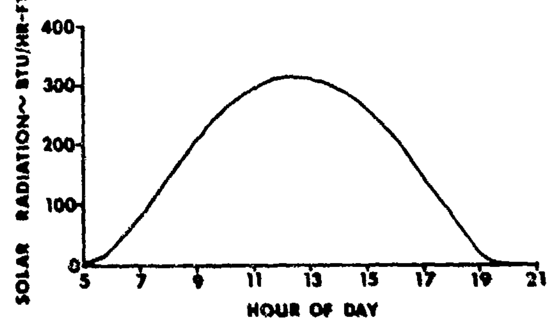

Figure 8. Daily Variation of Solar Radiation - Phoenix, Arizona (Ref 6).

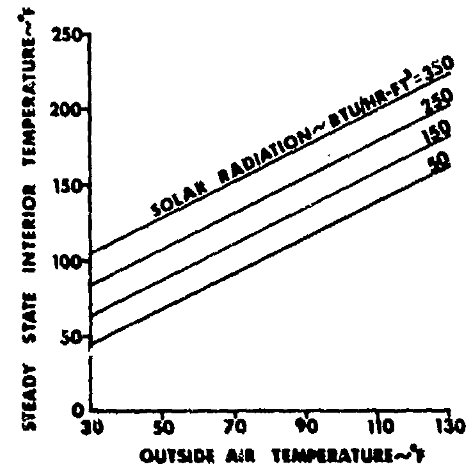

Figure 9. Static Interior Temperature.

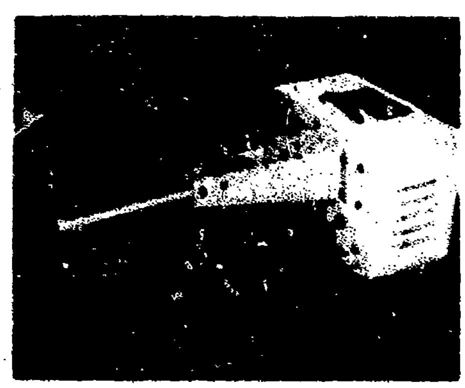

Figure 10. Thermal Radio ‹ter.

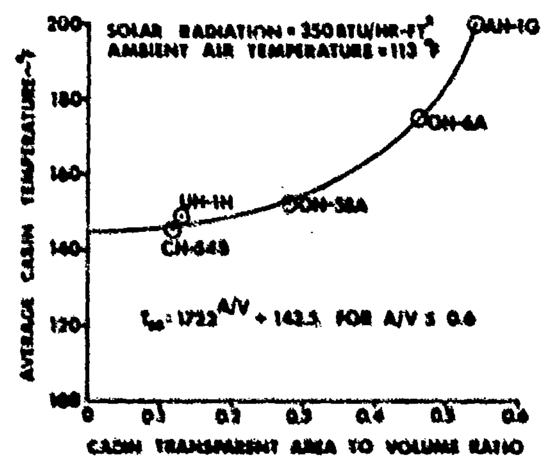

Figure 11. Cabin Static Temperature.

The test procedure consists of the following steps:

1. Aircraft cabin static temperatures are measured at mid-day and early-morning test conditions. The aircraft is parked so that it is directly facing the sun halfway through the mid-day test.

2. K_c and K_r are calculated using equations 4 and 5.

3. Aircraft cabin temperature is calculated from equation 2 at the desired values of ambient air temperature and solar radiation.

Different K_c and K_r coefficients are determined for each cabin location where the temperature is measured. A plot covering the full range of environmental conditions can be constructed as shown in figure 9.

Cabin temperature as a function of the daily cycle of solar radiation and ambient air temperature could not be measured because of the long response time of the cabin. Therefore, to check the accuracy of this test method, a small translucent plastic bottle was used to represent the aircraft cabin. The bottle had a volume of about 4 ounces and reached a steady-state temperature in about 10 minutes. This short response time allowed internal bottle temperatures to be recorded during the daily cycle of environmental conditions. Only a limited amount of data have been recorded over a temperature range of 45°F to 52°F and a solar radiation change of 63 to 162 BTU/hr-ft^2. The K_c and K_r coefficients remained constant for the plastic bottle for the conditions tested.

All presently available test data indicate that aircraft cabin static temperatures can be measured at conditions different than those desired and calculated for the desired conditions. To increase data validity, however, it is desirable to measure cabin static temperatures at environmental conditions as close to those desired as practical. For this test solar radiation was measured with a thermal radiometer, shown in figure 10, and cabin temperatures were recorded with a thermocouple system. For all calculations, temperatures are absolute in units of degrees Rankine. Test temperatures are measured in units of degrees Fahrenheit and converted to degrees Rankine. Final results are converted to units of degrees Fahrenheit.

TEST RESULTS

Table 2 presents cabin static temperatures at two upper cabin locations for each of the helicopters tested. These data were gathered at Edwards Air Force Base, California, which is located in the western Mojave high desert at an elevation of 2300 feet. Because of the altitude, the solar radiation at Edwards is about 50 BTU/hr-ft^2 higher and the ambient air temperature about 10°F lower than the corresponding values obtained at sea level western desert areas. The cabin temperatures

Table 2. Helicopter Upper Cabin Static Temperatures.

Designation	Standardized Data[1]		Test Data			
	Forward Cabin (~°F)	Aft Cabin (~°F)	Forward Cabin (~°F)	Aft Cabin (~°F)	Solar Radiation (BTU/hr-ft^2)	Ambient Air Temperature (~°F)
OH-58A	160	145	145	131	367	100
OH-6A	182	168	145	130	369	77.9
UH-1H	167	131	147	110	382	91.4
AH-1G	203	198	117	112	278	52.3
CH-54B	158	133	142	116	415	93

[1]Solar radiation: 350 BTU/hr-ft^2.
Ambient air temperature: 113°F.

are standardized to a solar radiation of 350 BTU/hr-ft^2 and an ambient air temperature of 113°F. Data were standardized to 350 BTU/hr-ft^2 and 113°F, since military specification MIL-STD-810B (ref 10) specifies these values for the conduct of test chamber solar radiation testing. The average of the forward and aft upper cabin temperatures is plotted versus the transparent area to cabin volume ratio in figure 11. The strong dependence of cabin static temperature on the area-to-volume ratio is clearly shown. The curve in figure 11 is empirically described by equation 6. This equation may be used to predict the approximate maximum static temperatures for aircraft and provide temperature environment design information for equipment located in the cabin area.

$$T_{ss} = 1722^{A/V} + 143.5, \text{ for } A/V \leq 0.6 \qquad (6)$$

All testing was conducted with an average wind speed of 5 knots or less. Wind caused lower cabin temperatures due to increased heat conduction from the cabin surface to the atmosphere with increasing wind speed. Aircraft were tested with all cabin vents, windows, and doors closed and with those cabin vents, windows, and doors open which could be left open with the aircraft parked unattended. Test results with the cabin open were strongly dependent on the wind speed. There was little or no difference in cabin temperatures between open and closed conditions with no wind and an increasing difference in temperatures with increasing wind speed. For an average wind speed of 5 knots, the only aircraft which showed a significant drop in cabin temperature with the cabin open was the UH-1H. A temperature drop of 7°F was recorded with the vents and windows open and 32°F with the vents, windows, and doors open. On all other aircraft tested, doors and windows could not be secured in a sufficiently open position to provide enough ventilation to reduce cabin temperatures. Opening of cabin vents was ineffective. Aircraft cabin heat transfer coefficients should be calculated only for closed cabin conditions.

The majority of United States Army avionics equipment is qualified to a continuous operating temperature range of -65°F to 131°F, an intermittent operating temperature range to 160°F, and a nonoperating temperature range of -80°F to 185°F (ref 11). No qualification is required for the transient condition which occurs when an aircraft cabin temperature is statically above the intermittent operating temperature limit, the aircraft cabin is open, and the aircraft immediately flown. This transient condition may cause avionics and equipment failures during the time required for cabin and equipment temperatures to cool to operating limits. Equipment should be tested for operation at the transient temperatures encountered when an aircraft goes from static to operating conditions. The data for the AH-1G helicopter indicate that the maximum nonoperating equipment temperature should be extended from 185°F to 203°F.

This test method has also been used for other enclosed areas of the aircraft where no transparent area is present and found to be valid. Although it has not been used for the measurement of surface temperatures, it should produce valid results. Static temperature information for many locations in each of the aircraft tested is presented in references 1 through 5.

CONCLUSIONS

This paper has described a new test method for the measurement of aircraft cabin static temperatures and has presented static temperature measurement data for the current generation of Army helicopters. It has been shown that:

1. Extreme values of solar radiation and ambient air temperature are not necessary to determine an aircraft static temperature environment. The test method presented in this paper allows measurement of static temperatures at the prevailing conditions and calculation of the aircraft static temperatures at the desired conditions.

2. The ratio of aircraft cabin transparent area to cabin volume can be used to predict approximate aircraft cabin static temperatures.

3. Aircraft equipment should be tested for operation at the transient temperatures encountered when an aircraft goes from static to operating conditions.

4. Maximum nonoperating equipment temperatures should be extended from 185°F to 203°F.

REFERENCES

1. USAASTA Final Report No. 70-15-1, *Instrument Panel and Avionics Compartment Environmental Survey, Production OH-58A Helicopter*, Laing, E. J., et al, US Army Aviation Systems Test Activity, September 1972.

2. USAASTA Final Report No. 70-15-2, *Vibration and Temperature Survey, Production UH-1H Helicopter*, Laing, E. J., et al, US Army Aviation Systems Test Activity, January 1973.

3. USAASTA Final Report No. 70-15-3, *Vibration and Temperature Survey, CH-54B Helicopter*, Laing, E. J., et al, US Army Aviation Systems Test Activity, March 1973.

4. USAASTA Final Report No. 70-15-4, *Vibration and Temperature Survey, Production OH-6A Helicopter*, Laing, E. J., et al, US Army Aviation Systems Test Activity, June 1973.

5. USAASTA Final Report, No. 70-15-5, *Vibration and Temperature Survey, Production AH-1G Helicopter*, Laing, E. J., et al, US Army Aviation Systems Test Activity, June 1974.

6. Publication, D2-905772-2, Atlas, R. A., and Charles, B. N., *Summary of Solar Radiation Characteristics, Tabular Summaries*, December 1964.

7. Publication, Instut Royale Meteorologique de Belgique, *Donnes du Rayonnement Solaire a Leopoldville, Periode 1953-1962*, 1965.

8. Publication, Report No. 21, *World Distribution of Solar Radiation*, Lof, George O. G., et al, Solar Energy Laboratory, University of Wisconsin, July 1966.

9. USATECOM Final Report, No. 9-CO-005-000-006, *Methodology Investigation of Joint USAECOM/USATECOM Solar Radiation Test of Selected USAECOM Equipments*, San Martin, R. L., US Army Test and Evaluation Command, March 1971.

10. Military Standard, MIL-STD-810B, *Environmental Test Methods*, 15 June 1967.

11. Military Specification, MIL-E-5400N, *Electronic Equipment, Airborne; General Specification For*, 30 November 1971.

A